Asymmetric nuclear matter studied by time-dependent local isospin density approximation

Enrico Lipparini* and Francesco Pederiva†

Dipartimento di Fisica, University of Trento, via Sommarive 14, I-38123 Povo, Trento, Italy
and INFN-TIFPA, Trento Institute of Fundamental Physics and Applications, Trento, Italy

(Received 6 May 2013; published 20 August 2013)

The dynamic response of asymmetric nuclear matter is studied by means of a time-dependent local isospin density approximation (TDLIDA) approach. Calculations are based on a local density energy functional derived by an auxiliary field diffusion Monte Carlo (AFDMC) calculation of bulk nuclear matter. Three types of excited states emerge: collective states, a continuum of quasiparticle-quasihole excitations and unstable solutions. These states are analyzed and discussed for different values of the nuclear density ρ and isospin asymmetry $\xi = (N - Z)/A$. An analytical expression of the compressibility as a function of ρ and ξ is derived which shows explicitly an instability of the neutron matter around $\rho \simeq 0.09$ fm^{-3} when a small fraction of protons are added to the system.

DOI: 10.1103/PhysRevC.88.024318 PACS number(s): 21.65.Cd, 21.60.Jz, 26.60.Dd

I. INTRODUCTION

The dynamic response function and the dynamic structure factor of nuclear matter at β equilibrium are key ingredients to understand several mechanisms related to interaction processes occurring in the interior of neutron stars. As it is well known since the seminal works of Sawyer [1,2], the structure factor is related to the mean free path of neutrinos in the nuclear medium [3]. The opacity of nuclear matter to neutrinos, and its implication in the neutrino emission in the early phases of existence of a neutron star, have been widely reviewed in the paper of Burrows *et al.* [4].

Another interesting piece of information that can be extracted from the knowledge of the dynamic structure factor concerns the mechanical instability of the system, that can be related to divergences in the response function and to a nonphysical negative value of the compressibility. This analysis becomes particularly interesting at values of the density where homogeneous matter is supposed to give way to more exotic inhomogeneous phases, before reaching the regime in which neutron-rich nuclei are dominant [4,5]. An interesting attempt to compute the structure factor of neutron matter by means of semiclassical simulations in this regime was recently performed by Horowitz *et al.* [6,7].

In general, several calculations of the low momentum structure factor of neutron matter have been performed using different methods. In particular we want to mention the results based on Brueckner-Hartree-Fock and random phase approximation theories, both at zero and finite temperature [8], and on the Landau theory approach starting from correlated basis functions effective interactions [9].

In this paper we propose a different route to the computation of the dynamic structure factor in the isoscalar and isovector channels for infinite nuclear matter with an arbitrary asymmetry.

The approach is based on first deriving a reasonable isospin-density functional from an equation of state (EoS) computed by means of the auxiliary field diffusion Monte Carlo (AFDMC) [10] method by Gandolfi *et al.* [11]. In that paper the EoS is derived from a density-dependent interaction, effectively including many-body contributions. This Hamiltonian was fitted to correctly reproduce the saturation properties of symmetric nuclear matter. The corresponding predictions of the EoS of pure neutron matter and matter at β equilibrium, including both electrons and muons, yield realistic values of quantities of astrophysical interest such as the mass/radius relation of a neutron star, in the same range of accuracy of, i.e., the well known Akmal-Pandharipande-Ravenhall (APR) EoS [12].

Obviously the range of densities that can be safely investigated relying on this EoS is limited. In the low-density limit symmetric nuclear matter becomes unstable, and neutron matter should be described including pairing correlations [13]. At densities of order $2\rho_0$, where $\rho_0 = 0.16$ fm^{-3} is the nuclear matter saturation density, one can expect the onset of hypernuclear degrees of freedom [14], or the transition to exotic matter phases which completely changes the scenario.

The obtained isospin-density functional is then used in a generalized linear response framework based on the time-dependent local density approximation (TDLDA). Following the idea of the local spin density approximation (LSDA; see, e.g., [15]), and its extension to the study of the dynamics of the system [16], we derive the response function in a time-dependent local isospin approximation (TDLIDA), and compute all the relevant physical quantities such as the frequency and strength of the collective modes and the compressibility for various values of the density and of the asymmetry at $T = 0$.

The paper is organized as follows. In Sec. II we will introduce in detail the derivation of the energy density functional; in Sec. II the extension of the TDLDA to the case of excitation in the isovector channel is discussed; Sec. IV contains the description of the results, and Sec. IV is devoted to conclusions.

II. DERIVATION OF THE ENERGY DENSITY FUNCTIONAL

By following the Kohn-Sham method [17], we introduce the local isospin density approximation (LIDA) for nuclear

*lipparin@science.unitn.it
†pederiva@science.unitn.it

matter defining the energy functional as

$$E(\rho,\xi) = T_0(\rho,\xi) + \int \epsilon_V(\rho,\xi)\rho\, d\mathbf{r}, \tag{1}$$

where $T_0(\rho,\xi)$ is the kinetic energy of the noninteracting system with density $\rho(\mathbf{r}) = \rho_n(\mathbf{r}) + \rho_p(\mathbf{r})$ and isospin polarization $\xi = \rho_1/\rho$ with $\rho_1(\mathbf{r}) = \rho_n(\mathbf{r}) - \rho_p(\mathbf{r})$, and where ρ_n and ρ_p are the neutron and proton densities, respectively. Note that T_0 is the kinetic energy of the noninteracting system, therefore it is missing the contributions related to dynamical quantum correlations. However, it has a comparable magnitude and is consistently treated in this method. Equation (1) defines the interaction-correlation energy per particle $\epsilon_V(\rho,\xi)$ of the asymmetric nuclear matter with density ρ and isospin polarization ξ. This quantity can be extracted by any independent calculation of the total energy per particle of asymmetric nuclear matter after subtraction of the free kinetic energy contributions at each value of ρ and ξ.

In this work we will use for $\epsilon_V(\rho,\xi)$ the following parametrization based on the auxiliary field diffusion Monte Carlo (AFDMC) calculations of Ref. [11]:

$$\epsilon_V(\rho,\xi) = \epsilon_0(\rho) + \xi^2\left[\epsilon_1(\rho) - \epsilon_0(\rho)\right], \tag{2}$$

where

$$\epsilon_q(\rho) = \epsilon_q^0 + a_q(\rho-\rho_0) + b_q(\rho-\rho_0)^2 + c_q(\rho-\rho_0)^3 e^{\gamma_q(\rho-\rho_0)} \tag{3}$$

are the interaction correlation energies of symmetric nuclear ($\xi = 0, q = 0$) and neutron matter ($\xi = 1, q = 1$), respectively. We have assumed the saturation density value $\rho_0 = 0.16$ fm^{-3}. The values of the parameters in Eq. (3) we have extracted from the fit are given in Table I.

The parametrization (2) reproduces very well the AFDMC calculations in a wide range of densities ρ (from $\rho_0/2$ to $3\rho_0$) and polarizations ξ.

By minimizing the energy functional (1) with the constraint that the number of neutrons and protons remains constant, we can derive a set of self-consistent equations by exactly treating the kinetic energy functional T_0. The detailed derivation can be found in Ref. [18]. The resulting set of coupled self-consistent equations for neutron and protons wave functions, assuming $\hbar = c = 1$, is given by

$$\left[-\frac{1}{2m}\nabla_{\mathbf{r}}^2 + v(\mathbf{r}) + w(\mathbf{r})\eta_\tau\right]\varphi_i^\tau(\mathbf{r}) = \varepsilon_{i,\tau}\,\varphi_i^\tau(\mathbf{r}), \tag{4}$$

TABLE I. Coefficients of the parametrization of the interaction-correlation energy of symmetric nuclear matter ($q = 0$) and pure neutron matter ($q = 1$) derived by fitting the equation of state of Ref. [11].

q	ϵ_q^0 (MeV)	a_q (MeV fm^3)	b_q (MeV fm^6)	c_q (MeV fm^9)	γ_q (fm^3)
0	−38.1	−92.1	630.1	−1717.2	−2.360
1	−19.8	−21.0	533.0	−1327.7	−2.201

where i stands for the set of quantum numbers, excluding isospin, that characterize the single-particle wave functions. The nuclear neutron and proton densities are given by

$$\rho_\tau = \sum_i \left|\varphi_i^\tau(\mathbf{r})\right|^2$$

with $\eta_\tau = 1(-1)$ if $\tau = n(p)$ and n, p stands for neutrons and protons, respectively. The effective potentials in Eq. (4) are derived from the interaction-correlation energy functional deriving with respect to the density and isospin polarization:

$$v(\mathbf{r}) = \frac{\partial\rho\epsilon_V[\rho(\mathbf{r}),\xi]}{\partial\rho(\mathbf{r})}, \quad w(\mathbf{r}) = \frac{\partial\epsilon_V[\rho(\mathbf{r}),\xi)]}{\partial\xi(\mathbf{r})}. \tag{5}$$

As it is well known, the Kohn-Sham method sketched here gives an exact solution of the variational principle which minimizes the energy functional (1). The theory is still approximate in the sense that the exact interaction-energy functional is unknown, and one needs to rely on some expression derived by independent calculations. Concerning our choice for $\epsilon_V(\rho,\xi)$, we want to point out again that the functional (1), as discussed in Ref. [11], gives an equation of state of asymmetric nuclear matter providing realistic predictions for neutron stars properties when the β-equilibrium condition is imposed. We can therefore be confident that both the density and isospin polarization dependence are sufficiently accurate to yield reasonable values also for the first and second derivatives of ϵ_V with respect to ρ and ξ. These are the main ingredients of the Kohn-Sham method and of its time-dependent version described in the next section.

Finally, we notice that, when applied to infinite nuclear matter, the static equations (4) are satisfied by plane-wave solutions for $\varphi_i^\tau(\mathbf{r})$, since in this case all the densities are constant as well as the density-dependent potentials (5). As a consequence, the Kohn-Sham equilibrium density and energy per particle are obviously the same as that of the starting interaction used to derive the energy functional. Hence, the static Kohn-Sham equations do not give any information in infinite systems. However, as described in the next section, the *time-dependent* versions of them give new and useful solutions for the nuclear response even starting from the same simple ingredients.

III. TDLIDA RESPONSE OF INFINITE ASYMMETRIC NUCLEAR MATTER

In this section we derive the TDLIDA density-density $[\chi^s(q,\omega)]$ and isovector-density/isovector-density $[\chi^v(q,\omega)]$ response functions of a three-dimensional (3D), spin-unpolarized, uniform gas of N neutrons and Z protons ($N + Z = A$), with isospin polarization $\xi = \rho_1/\rho$.

We start writing the time-dependent Kohn-Sham (KS) equations in an external, time-dependent field along the $\mathbf{r}$ direction:

$$\sum_{k=1}^{A}\lambda_\tau^k\left(e^{i(\mathbf{q}\cdot\mathbf{r}_k-\omega t)} + e^{-i(\mathbf{q}\cdot\mathbf{r}_k-\omega t)}\right), \tag{6}$$

with $\lambda_\tau^k = \lambda$ for density excitations and $\lambda_\tau^k = \lambda\eta_\tau$ for isovector-density excitations. The KS equations read

$$i\frac{\partial}{\partial t}\varphi_i^\tau(\mathbf{r},t) = \Big\{-\frac{1}{2m}\nabla_\mathbf{r}^2 + +v[\rho_n(\mathbf{r},t),\rho_p(\mathbf{r},t)] + w[\rho_n(\mathbf{r},t),\rho_p(\mathbf{r},t)]\eta_\tau + \lambda_\tau[e^{i(\mathbf{q}\cdot\mathbf{r}-\omega t)} + e^{-i(\mathbf{q}\cdot\mathbf{r}-\omega t)}]\Big\}\varphi_i^\tau(\mathbf{r},t). \quad (7)$$

In the uniform 3D nucleon gas, the nuclear density oscillations induced by the external field are given by

$$\rho_n(\mathbf{r},t) = \rho_n + \delta\rho_n(\mathbf{r},t), \quad \rho_p(\mathbf{r},t) = \rho_p + \delta\rho_p(\mathbf{r},t), \quad (8)$$

where ρ_n and ρ_p are the neutron and proton constant densities of the unperturbed initial state, respectively, and

$$\delta\rho_n(\mathbf{r},t) = \delta\rho_n(e^{i(\mathbf{q}\cdot\mathbf{r}-\omega t)} + e^{-i(\mathbf{q}\cdot\mathbf{r}-\omega t)}), \quad \delta\rho_p(\mathbf{r},t) = \delta\rho_p(e^{i(\mathbf{q}\cdot\mathbf{r}-\omega t)} + e^{-i(\mathbf{q}\cdot\mathbf{r}-\omega t)}), \quad (9)$$

as follows from translational invariance. The quantities $\delta\rho_n$ and $\delta\rho_p$ are constants to be determined. Equations (7) and (9) have solutions describing density fluctuations in the density operator $F = \sum_{k=1}^A e^{i\mathbf{q}\cdot\mathbf{r}_k}$, and isovector-density operator $F_\tau = \sum_{k=1}^A e^{i\mathbf{q}\cdot\mathbf{r}_k}\eta_\tau^k$, given by

$$\delta F(\hat{O},\omega) = \langle\psi(t)|F|\psi(t)\rangle - \langle 0|F|0\rangle = \int d\mathbf{r}\, e^{i\mathbf{q}\cdot\mathbf{r}}[\rho(\mathbf{r},t)-\rho]_{\hat{O}} = V\, e^{i\omega t}(\delta\rho_n + \delta\rho_p), \quad (10)$$

and

$$\delta F_\tau(\hat{O},\omega) = \langle\psi(t)|F_\tau|\psi(t)\rangle - \langle 0|F_\tau|0\rangle = \int d\mathbf{r}\, e^{i\mathbf{q}\cdot\mathbf{r}}[\rho_1(\mathbf{r},t)-\rho_1]_{\hat{O}} = V\, e^{i\omega t}(\delta\rho_n - \delta\rho_p), \quad (11)$$

where V is the volume of the gas and $\hat{O} = \sum_{k=1}^A e^{-i\mathbf{q}\cdot\mathbf{r}_k}$.

The density-density response is given by [18]

$$\chi^s(q,\omega) = \frac{V(\delta\rho_n + \delta\rho_p)}{\lambda} \equiv \chi^n(q,\omega) + \chi^p(q,\omega), \quad (12)$$

and the isovector-density/isovector-density response is

$$\chi^v(q,\omega) = \frac{V(\delta\rho_n - \delta\rho_p)}{\lambda} \equiv \chi^n(q,\omega) - \chi^p(q,\omega). \quad (13)$$

In order to determine $\delta\rho_n$ and $\delta\rho_p$, we then insert $\rho_n(\mathbf{r},t)$, $\rho_p(\mathbf{r},t)$ of Eqs. (8) and (9) into (7) and linearize the equations. This procedure determines the self-consistent KS mean-field potential entering Eq. (7) to be

$$V_{KS}[\rho_n(\mathbf{r},t),\rho_p(\mathbf{r},t)] = V_{KS}(\rho_n,\rho_p) + \frac{\partial V_{KS}}{\partial\rho_n(\mathbf{r},t)}\Big|_{\rho_n,\rho_p}\delta\rho_n(\mathbf{r},t) + \frac{\partial V_{KS}}{\partial\rho_p(\mathbf{r},t)}\Big|_{\rho_n,\rho_p}\delta\rho_p(\mathbf{r},t). \quad (14)$$

Eventually, from Eqs. (7) and (14) we obtain

$$i\frac{\partial}{\partial t}\varphi_i^n(\mathbf{r},t) = \Big\{-\frac{1}{2m}\nabla_\mathbf{r}^2 + \text{const.} + [\delta\rho_n V_{n,n} + \delta\rho_p V_{n,p} + \lambda] \times (e^{i(\mathbf{q}\cdot\mathbf{r}-\omega t)} + e^{-i(\mathbf{q}\cdot\mathbf{r}-\omega t)})\Big\}\varphi_i^n(\mathbf{r},t),$$
$$i\frac{\partial}{\partial t}\varphi_i^p(\mathbf{r},t) = \Big\{-\frac{1}{2m}\nabla_\mathbf{r}^2 + \text{const.} + [\delta\rho_n V_{n,p} + \delta\rho_p V_{n,n} \pm \lambda] \times (e^{i(\mathbf{q}\cdot\mathbf{r}-\omega t)} + e^{-i(\mathbf{q}\cdot\mathbf{r}-\omega t)})\Big\}\varphi_i^p(\mathbf{r},t), \quad (15)$$

where in the second equation one must keep the plus sign when calculating the density-density response, and the minus sign when calculating the isovector-density/isovector-density response. In Eqs. (15) we have defined the mean-field potentials

$$V_{nn} = \frac{\partial(v+w)}{\partial\rho_n(\mathbf{r},t)}\Big|_{\rho_n,\rho_p} = \left(\frac{\partial}{\partial\rho} + \frac{1}{\rho}\frac{\partial}{\partial\xi}\right)(v+w)\Big|_{\rho,\xi},$$
$$V_{np} = \frac{\partial(v+w)}{\partial\rho_p(\mathbf{r},t)}\Big|_{\rho_n,\rho_p} = \left(\frac{\partial}{\partial\rho} - \frac{1}{\rho}\frac{\partial}{\partial\xi}\right)(v+w)\Big|_{\rho,\xi},$$
$$V_{pn} = \frac{\partial(v-w)}{\partial\rho_n(\mathbf{r},t)}\Big|_{\rho_n,\rho_p} = \left(\frac{\partial}{\partial\rho} + \frac{1}{\rho}\frac{\partial}{\partial\xi}\right)(v-w)\Big|_{\rho,\xi}, \quad (16)$$
$$V_{pp} = \frac{\partial(v-w)}{\partial\rho_p(\mathbf{r},t)}\Big|_{\rho_n,\rho_p} = \left(\frac{\partial}{\partial\rho} - \frac{1}{\rho}\frac{\partial}{\partial\xi}\right)(v-w)\Big|_{\rho,\xi}.$$

Equations (15) can be rewritten as

$$i\frac{\partial}{\partial t}\varphi_i^n(\mathbf{r},t) = \Big\{-\frac{1}{2m}\nabla_\mathbf{r}^2 + C + \lambda_n'[e^{i(\mathbf{q}\cdot\mathbf{r}-\omega t)} + e^{-i(\mathbf{q}\cdot\mathbf{r}-\omega t)}]\Big\}\varphi_i^n(\mathbf{r},t),$$
$$i\frac{\partial}{\partial t}\varphi_i^p(\mathbf{r},t) = \Big\{-\frac{1}{2m}\nabla_\mathbf{r}^2 + C + \lambda_p'[e^{i(\mathbf{q}\cdot\mathbf{r}-\omega t)} + e^{-i(\mathbf{q}\cdot\mathbf{r}-\omega t)}]\Big\}\varphi_i^p(\mathbf{r},t), \quad (17)$$

where C is a constant, and

$$\lambda_n' = \delta\rho_n V_{n,n} + \delta\rho_p V_{n,p} + \lambda, \quad \lambda_p' = \delta\rho_n V_{p,n} + \delta\rho_p V_{p,p} \pm \lambda. \quad (18)$$

Equation (17) coincides with that of a noninteracting system coupled to an external time oscillating field, with a coupling constant λ' given by Eq. (18). For such a system, the density response functions are the single-particle free responses $\chi_0^n(q,\omega)$, $\chi_0^p(q,\omega)$. From Eqs. (12) and (13) and from the analogous relations for the free response functions

$$\chi_0^n(q,\omega) = \frac{V\delta\rho_n}{\lambda_n'}, \quad \chi_0^p(q,\omega) = \frac{V\delta\rho_p}{\lambda_p'} \quad (19)$$

we obtain

$$\lambda\,\chi^n(q,\omega) = \lambda_n'\,\chi_0^n(q,\omega) = L\delta\rho_n, \quad \lambda\,\chi^p(q,\omega) = \lambda_p'\,\chi_0^p(q,\omega) = L\delta\rho_p. \quad (20)$$

The solution of these equations, finally gives the TDLIDA response functions

$$\chi^s = V\frac{\chi_0^n\big[V-(V_{p,p}-V_{n,p})\chi_0^p\big]+\chi_0^p\big[V-(V_{n,n}-V_{p,n})\chi_0^n\big]}{\big(V-V_{p,p}\chi_0^p\big)\big(V-V_{n.n}\chi_0^n]\big)-V_{n,p}\chi_0^n V_{p,n}\chi_0^p},$$
$$\chi^v = V\frac{\chi_0^n\big[V-(V_{p,p}+V_{n,p})\chi_0^p\big]+\chi_0^p\big[V-,(V_{n,n}+V_{p,n})\chi_0^n\big]}{\big(V-V_{p,p}\chi_0^p\big)\big(V-V_{n,n}\chi_0^n\big)-V_{n,p}\chi_0^n V_{p,n}\chi_0^p}. \tag{21}$$

Equations (21) allow study of the response of partially isospin-polarized nuclear matter ($N \neq Z$), which is the aim of the present work.

Note that for fully isospin-unpolarized systems ($N = Z$) the above equations are drastically simplified. In fact, in this case, one has $\rho_n = \rho_p = \rho/2$, $\chi_0^n = \chi_0^p = \chi_0/2$ and $V_{n,n} = V_{p,p} = (\frac{\partial v}{\partial \rho} + \frac{1}{\rho}\frac{\partial w}{\partial \xi})|_{\rho,\xi=0}$, $V_{n,p} = V_{p,n} = (\frac{\partial v}{\partial \rho} - \frac{1}{\rho}\frac{\partial w}{\partial \xi})|_{\rho,\xi=0}$ and one gets from Eqs. (21)

$$\chi^s(q,\omega) = \frac{\chi_0(q,\omega)}{1-\frac{\partial v}{\partial \rho}\big|_{\rho,\xi=0}\frac{\chi_0(q,\omega)}{V}}, \tag{22}$$

and

$$\chi^v(q,\omega) = \frac{\chi_0(q,\omega)}{1-\frac{1}{\rho}\frac{\partial w}{\partial \xi}\big|_{\rho,\xi=0}\frac{\chi_0(q,\omega)}{V}}, \tag{23}$$

which have the same form of the RPA responses of isospin unpolarized systems, but not the same meaning, since they have as main ingredients the derivative of the self-consistent KS potentials, and not the Fourier transform of an effective nucleon-nucleon interaction as in the RPA theory.

The same simplifications occur in the case of pure neutron matter. In this case one finds that $\chi_0^p = 0$. Consequently,

$$\chi^s(q,\omega) = \chi^v(q,\omega) = \frac{\chi_0^n(q,\omega)}{1-V_{n,n}\frac{\chi_0^n(q,\omega)}{V}}. \tag{24}$$

Since the time-dependent density functional approach only holds in the low-q, low-ω limits [18], in the following we will use as the free response functions χ_0^n and χ_0^p entering Eqs. (21) the following simple expressions valid in these limits:

$$\chi_0^{n,p}(\mathbf{q},\omega) = -V\nu^{n,p}\left[1+\frac{s}{2(1\pm\xi)^{1/3}}\ln\frac{s-(1\pm\xi)^{1/3}}{s+(1\pm\xi)^{1/3}}\right], \tag{25}$$

where $\nu^{n,p} = mk_F^{n,p}/\pi^2 = mk_F(1\pm\xi)^{1/3}/\pi^2$, $k_F = (\frac{3\pi^2}{2}\rho)^{1/3}$, $s = \omega/(qv_f)$. The plus sign holds for χ_0^n and the minus sign for χ_0^p. Note that in the low-q, low-ω limits, χ_0^n and χ_0^p depend on q and ω only through the combination $s = \omega/(qv_f)$. Since $\chi^{s,v}$ of Eqs. (21) depends on q and ω only via the dependence of χ_0^n and χ_0^p on these variables, also the interacting responses turn out to be functions of s only. As in Landau theory, also in TDLIDA the nuclear responses are functions of $s = \omega/(qv_f)$ and not of q and ω separately.

IV. RESULTS

A. Mean-field potential

From Eqs. (21), by taking the imaginary part of χ, it is possible to calculate the excitation strength $S^{s,v}(q,\omega) = -(1/\pi)\,\mathrm{Im}\,\chi^{s,v}$ and the moments $m_k^{s,v}$ of the density (s) and isovector density (v) excitation operators $F^{s,v}$, with $F^s = \sum_{k=1}^A e^{i\mathbf{q}\cdot\mathbf{r}_k}$ and $F^v = \sum_{k=1}^A e^{i\mathbf{q}\cdot\mathbf{r}_k}\eta_\tau^k$. The moments are given by

$$m_k^{s,v} = \int_0^\infty d\omega\,\omega^k S^{s,v}(q,\omega) = \sum_n \omega_{no}^k|\langle 0|F^{s,v}|n\rangle|^2. \tag{26}$$

By setting the mean-field potentials V_{nn}, V_{pp}, V_{np} equal to zero it is possible to write

$$S_{\rm free}^{s,v}(q,\omega) = \frac{Vmk_F}{\pi^2}\frac{s}{2}\left[\Theta\left(1-\frac{s}{(1+\xi)^{1/3}}\right)+\Theta\left(1-\frac{s}{(1-\xi)^{1/3}}\right)\right], \tag{27}$$

which gives the one-particle–one-hole excitation strength, and, by integration, the Fermi gas energy moments of the asymmetric noninteracting nuclear matter.

In Figs. 1–3 and Tables II–IV thevalues of the adimensional interaction parameters $G_n = \nu_n V_{nn}$, $G_p = \nu_p V_{pp}$, and $G_{np} = \sqrt{\nu_n\nu_p}V_{np}$ are reported as a function of the isovector polarization $\xi = (N-Z)/A$ for three values of the density ρ. These quantities show a strong ξ and ρ dependence, giving rise to excitations strengths and moments which are quite different from the non interacting cases.

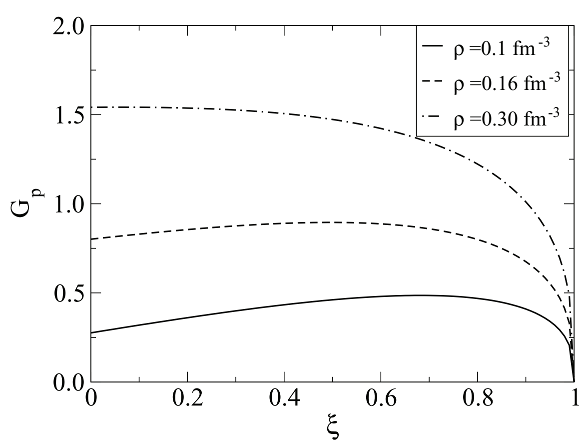

FIG. 1. Adimensional interaction parameter $G_p = \nu_p V_{pp}$ as a function of the isospin asymmetry $\xi = (N-Z)/A$ for three different values of the density ρ.

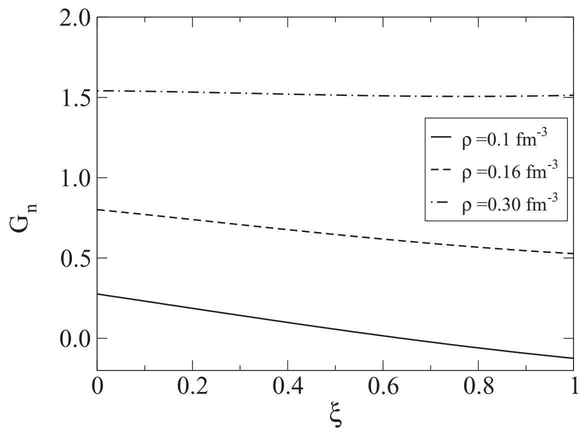

FIG. 2. Same as in Fig. 1 for the interaction parameter $G_n = \nu_n V_{nn}$.

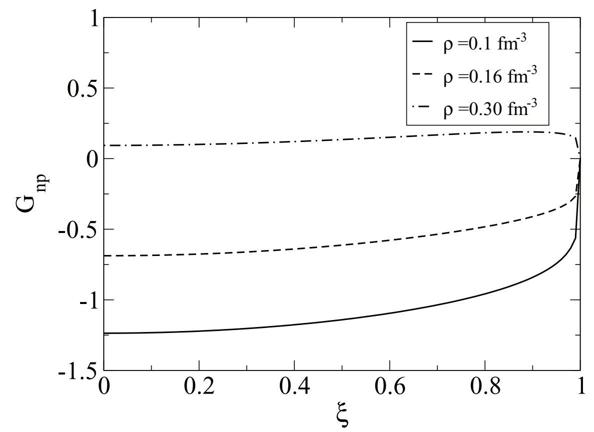

FIG. 3. Same as in Fig. 1 for the interaction parameter $G_{np} = \sqrt{\nu_n \nu_p} V_{np}$.

B. Energy-weighted sum rules

We first consider the moments m_{-1}, m_1, m_3 of the density (s) and isovector density (v) operators, F^s and F^v. These quantities still have analytical expressions, given by

$$m_{-1}^{s,v} = \frac{V}{2} \frac{\nu_n(1+G_p) + \nu_p(1+G_n) \mp 2\sqrt{\nu_p \nu_n} G_{np}}{(1+G_p)(1+G_n) - G_{np}^2}, \quad (28)$$

$$m_1^{s,v} = \frac{N}{2} \frac{q^2}{m}, \quad (29)$$

$$m_3^{s,v} = \frac{V}{2} \frac{q^4}{m^8} \left\{ \frac{1}{5} \left(\nu_n^5 + \nu_p^5\right) + \frac{1}{9} \left[\nu_n^5 G_n + \nu_p^5 G_p \pm 2\nu_n^{5/2} \nu_p^{5/2} G_{np}\right] \right\}, \quad (30)$$

where the minus sign applies to density excitations and the plus sign to the isovector-density ones.

The m_{-1} moment is known as the *hydrodynamic sum rule* because in the $N = Z$ case it is directly related to ordinary sound velocity. The m_1 moment is the f-sum rule, and the m_3 moment is related to the elastic properties of the Fermi systems (for a wide illustration of the properties of these sum rules see Ref. [18]). In the case of pure neutron matter, the m_{-1} moment is related to the neutron matter compressibilty K^n by the relation

$$\frac{m_{-1}}{m_{-1}^0} = \frac{K^n}{K_0^n} = \frac{1}{1+G_n}, \quad (31)$$

where $m_{-1}^0 = V\nu_n/2$ and $K_0^n = 9\pi^2 m/k_F^{n5}$ respectively are the Fermi gas static polarizability and compressibility. Similar expressions also hold in the symmetric nuclear matter ($N = Z$), where $\nu_n = \nu_p$, and $G_p = G_n = G$. In this case the moments read

$$\frac{m_{-1}^s}{m_{-1}^0} = \frac{K}{K_0} = \frac{1}{1+G+G_{np}}, \quad (32)$$

and

$$\frac{m_{-1}^v}{m_{-1}^0} = \frac{1}{1+G-G_{np}}, \quad (33)$$

for the isoscalar and isovector cases, respectively. Expressions (31) and (32) are quite similar to the results of Landau theory for neutron and symmetric nuclear matter [18]. The true novelty of Eqs. (21) and (28)–(30) stands in their *explicit* dependence on N, Z which allows us to study the properties of the nuclear response when a fraction of protons is present in the neutron matter, as happens in the neutron star interior.

Note that, in the local isospin density approximation used here, the f-sum rule m_1 is the same for both the isoscalar and isovector excitation operators, whereas calculating m_1^v directly from the original interaction used to derive the local energy functional would have yielded for m_1^v an interaction contribution. This reflects a failure of the model in reproducing quantities in the high-ω region. The sum rules (28)–(30) are

TABLE II. Numerical results at density $\rho = 0.10$ fm^{-3} and various isospin polarizations for (a) the energy $\bar{s}$ of the collective mode in the isoscalar (s) or isovector (v) channels, and corresponding fraction of the f-sum rule exhausted by such modes; (b) the centroids of the collective peaks excitations predicted by the energy-weighted sum rules [see Eq. (34)]; and (c) interaction parameters giving the mean-field potential.

ξ	$\bar{s}_s$	% m_1^s	$\bar{s}_v$	% m_1^v	$s_{1,-1}^s$	$s_{1,-1}^v$	$s_{3,1}^s$	$s_{3,1}^v$	G_p	G_n	G_{np}
0.0			1.1036	81.4	0.115	0.915	0.529	1.051	0.2757	0.2757	−1.2363
0.3	1.1154	7.7	1.1154	58.2	0.142	0.925	0.472	1.088	0.3991	0.1422	−1.2031
0.5	1.1466	5.5	1.1466	15.1	0.183	0.890	0.472	1.131	0.4611	0.0561	−1.1409
0.8					0.269	0.891	0.564	1.105	0.4690	−0.0599	−0.9578
0.9					0.313	0.915	0.632	1.129	0.4093	−0.0937	−0.8408
1.0					0.681	0.681	0.942	0.942	0.0000	−0.1247	0.0000

TABLE III. Same as Table II for density $\rho = 0.16$ fm^{-3}.

ξ	$\bar{s}_s$	$\% \, m_1^s$	$\bar{s}_v$	$\% \, m_1^v$	$s^s_{1,-1}$	$s^v_{1,-1}$	$s^s_{3,1}$	$s^v_{3,1}$	G_p	G_n	G_{np}
0.0			1.1008	80.9	0.609	0.911	0.799	1.047	0.8012	0.8012	−0.6877
0.3	1.1316	17.8	1.1316	60.7	0.614	0.909	0.793	1.076	0.8759	0.7077	−0.6610
0.5	1.1685	26.8	1.1685	46.9	0.623	0.904	0.820	1.102	0.8953	0.6464	−0.6125
0.8	1.2281	29.6	1.2281	33.6	0.650	0.901	0.916	1.150	0.7997	0.5669	−0.4826
0.9	1.2481	29.1	1.2481	30.7	0.667	0.908	0.967	1.167	0.6751	0.5455	−0.4106
1.0	1.2680	28.5	1.2680	28.5	0.899	0.899	1.110	1.110	0.0000	0.5271	0.0000

only valid in the low-q and low-ω limits, where the TDLIDA is expected to work. They only account for one-particle–one-hole and collective excitations. Many-particle–many-hole excitations are important in the high-energy part of the excitation spectrum [19], and give an important contribution to m_1^v. Following this argument, since the m_{-1} moment is mainly determined by the low-energy part of the spectrum, one expects that this sum rule should be the closest to the the exact value that might in principle be computed by directly solving the many-body Schroedinger equation.

C. Collective modes and dynamic structure factors

We now turn to the interacting excitation strength $S(s = \omega/qv_F)$. The interaction produces new types of excitations beyond the usual one-particle–one-hole ones which are the only excitations of the noninteracting case. These excitations are given by the poles of the response functions (21), which are the solutions of the equations

$$(1 + G_p\Omega^p)(1 + G_n\Omega^n) - G^2_{n,p}\Omega^n\Omega^p = 0, \qquad (34)$$

where $\Omega^{n,p} = [1 + \frac{s}{2(1\pm\xi)^{1/3}} \ln \frac{s-(1\pm\xi)^{1/3}}{s+(1\pm\xi)^{1/3}}]$, with the plus sign holding for Ω^n and the minus sign for Ω^p. Depending on the strength of the interaction, these new solutions are essentially of three types: (a) real solutions such that $s > (1 \pm \xi)^{1/3}$ (collective modes), producing a discrete peak in the dynamic form factor $S(s)$ with no attenuation; (b) solutions with some imaginary component, and corresponding modes which decay by exciting single quasiparticle-quasihole pairs (Landau damping); and (c) unstable solutions which are associated with the divergence of the polarizability sum rules $m^{s,v}_{-1}$.

In Tables II–IV we report the values $\bar{s}$ of s at which the collective states occur in the isoscalar ($\bar{s}_s$) and isovector ($\bar{s}_v$) strengths, the percentage m_1^s and m_1^v of the energy-weighted sum rule exhausted by the collective states in the isoscalar and isovector channels, respectively, and the two mean s values

$$\bar{s}^{s,v}_{1,-1} = \frac{\omega^{s,v}_{1,-1}}{qv_F} = \sqrt{\frac{m_1^{s,v}}{m_{-1}^{s,v}}}\frac{1}{qv_F},$$
$$\bar{s}^{s,v}_{3,1} = \frac{\omega^{s,v}_{3,1}}{qv_F} = \sqrt{\frac{m_3^{s,v}}{m_1^{s,v}}}\frac{1}{qv_F}, \qquad (35)$$

obtained by Eqs. (28)–(30). The energy $\omega^{s,v}_{1,-1}$ is hereafter referred to as the *hydrodynamic* energy in analogy to what happens in liquid He^3, where $v_1 = \omega^s_{1,-1}/q$ reproduces the predictions of the hydrodynamical model for the ordinary (first-) sound wave. Conversely the energy $\omega^{s,v}_{3,1}$ is referred to as the *elastic* energy since in liquid He^3 $v_0 = \omega^s_{3,1}/q$ reproduces the predictions of the elastic model for the zero-sound wave [18].

The strength of the collective state at $s = \bar{s}$ can be computed from the following (adymensional) expression for the response:

$$\frac{\chi^{s,v}}{Nm/(2k_F^2)} = -3\frac{(1+\xi)^{1/3}\Omega^n\left[1+\left(G_p \mp \left(\frac{1-\xi}{1+\xi}\right)^{1/6}G_{np}\right)\Omega^p\right] + (1-\xi)^{1/3}\Omega^p\left[1+\left(G_n \mp \left(\frac{1+\xi}{1-\xi}\right)^{1/6}G_{np}\right)\Omega^n\right]}{(1+G_p\Omega^p)(1+G_n\Omega^n) - G^2_{n,p}\Omega^n\Omega^p}, \qquad (36)$$

TABLE IV. Same as Table II for density $\rho = 0.30$ fm^{-3}.

ξ	$\bar{s}_s$	$\% \, m_1^s$	$\bar{s}_v$	$\% \, m_1^v$	$s^s_{1,-1}$	$s^v_{1,-1}$	$s^s_{3,1}$	$s^v_{3,1}$	G_p	G_n	G_{np}
0.0	1.1188	83.6	1.0958	80.1	0.937	0.903	1.070	1.040	1.5414	1.5414	0.0935
0.3	1.2072	58.2	1.2072	48.0	0.943	0.902	1.099	1.059	1.5260	1.5267	0.1091
0.5	1.2643	64.3	1.2643	57.8	0.953	0.900	1.148	1.094	1.4732	1.5146	0.1351
0.8	1.3420	74.6	1.3420	71.7	0.986	0.902	1.263	1.188	1.2229	1.5064	0.1829
0.9	1.3666	78.0	1.3666	76.5	1.011	0.909	1.310	1.232	1.0106	1.5084	0.1893
1.0	1.3907	81.4	1.3907	81.4	1.153	1.153	1.324	1.324	0.0000	1.5134	0.0000

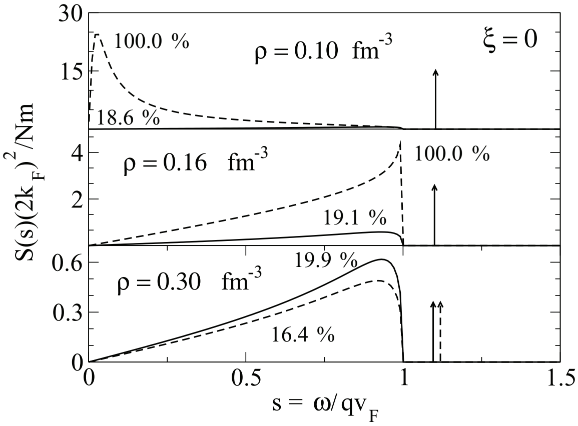

FIG. 4. Quasiparticle-quasihole excitation strengths in units of $Nm/2k_F^2$ as a function of $s = \omega/qv_F$ for three different values of the density ($\rho = 0.30$ fm^{-3}, $\rho = 0.16$ fm^{-3}, $\rho = 0.10$ fm^{-3}) at fixed isospin asymmetry $\xi = 0$. The positions of the collective states, when present, are indicated by an arrow. The dashed and full lines stand for the isoscalar and isovector excitation strengths, respectively. The fraction of the energy-weighted sum rule exhausted by the two strengths is also reported near the curves. The remaining fraction of the energy-weighted sum rule is exhausted by the collective states.

derived from Eqs. (21) and (25) by expanding $\chi^{s,v}$ around the pole at $\bar{s}$. Naming $N(s)$ and $D(s)$ the numerator and the denominator of Eq. (36), respectively, one obtains

$$\frac{S(s)}{Nm/\left(2k_F^2\right)} = \frac{N(s)}{\frac{\partial D(s)}{\partial s}}\delta(s-\bar{s}). \tag{37}$$

The fraction of the f-sum rule m_1 exhausted by the collective state is easily calculated to be

$$\bar{s}\frac{N(\bar{s})}{\frac{\partial D(s)}{\partial s}\Big|_{s=\bar{s}}}. \tag{38}$$

In Figs. 4–8 we then plot the quasi-particle-quasi-hole excitation strengths $S^{s,v}(s = \omega/qv_F)$ in units of $Nm/(2k_F^2)$ for different values of the density ρ and s at fixed values of the isospin polarization ξ. This quantity has been obtained by numerically computing the imaginary part of expression (36). In the figures the fraction of the energy-weighted sum rule exhausted by the continuum of quasi-single-particle states is explicitly indicated, and the position of the collective state, if present, is indicated by an arrow. In all the calculations presented in the following, we have numerically checked that the particle-hole and collective contributions to the strength completely exhaust the m_1 sum rule. Let us start the discussion of the two extreme cases corresponding to $\xi = 0$ (symmetric nuclear matter $N = Z$) and $\xi = 1$ (pure neutron matter $Z = 0$). In the first case ($N = Z$), isoscalar and isovector modes are decoupled in the sense that the isoscalar and isovector density operators F^s and F^v give rise to distinct isoscalar and isovector strengths $S^s(s = \omega/qv_F)$ and $S^v(s = \omega/qv_F)$. This is different from what happens when $N \neq Z$ where F^s and F^v can indifferently excite modes both in the isoscalar and in the isovector channels, with strengths and weights depending on the values of ξ and ρ. Obviously, for neutron

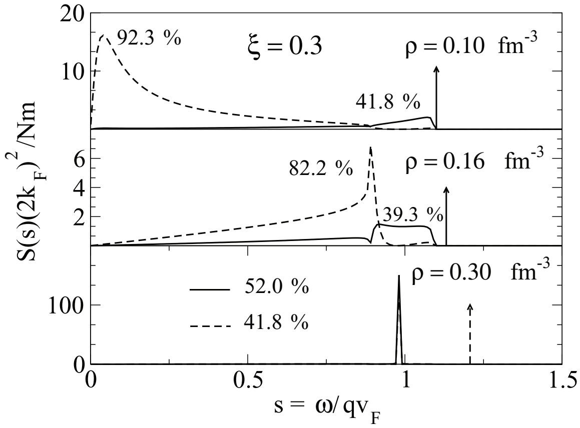

FIG. 5. Same as in Fig. 4 at isospin asymmetry $\xi = 0.3$. The collective state, indicated with an arrow, has the same energy both in the isoscalar and isovector channels. The dashed and full lines stand for the isoscalar and isovector excitation strengths, respectively. The fraction of the energy-weighted sum rule exhausted by the two strengths is also reported near the curves. The arrow is dashed or full depending on whether the collective state exhausts more strength in the isoscalar or in the isovector channel.

matter ($Z = 0$) it makes no sense to speak of isoscalar and isovector modes since in this case there is only one type of excitation.

For symmetric nuclear matter ($\xi = 0$) at density $\rho = 0.30$ fm^{-3}, in the isoscalar strength $S^s(s)$ a strong collective state is present at $\bar{s}_s = 1.1188$, exhausting about 83.6% of the energy-weighted sum rule m_1. A continuum of single-particle-type excitations is instead predicted at lower s values. A similar situation occurs for $S^v(s)$. Here the collective state is at at $\bar{s}_v = 1.0958$, and exhausts about 80.1% of the energy-weighted sum rule m_1. The collective states in both the cases occur at energies which are closer to the mean excitation energies $\omega_{3,1}^{s,v}$ than to the $\omega_{1,-1}^{s,v}$ ones, showing that the collective modes are of mainly of elastic type. This situation is analogous to what happens, for instance, in liquid He^3. By decreasing the density, we still predict the existence of a strong collective state in the isovector channel, exhausting about 80% of the energy-weighted sum rule m_1. On the other hand, the

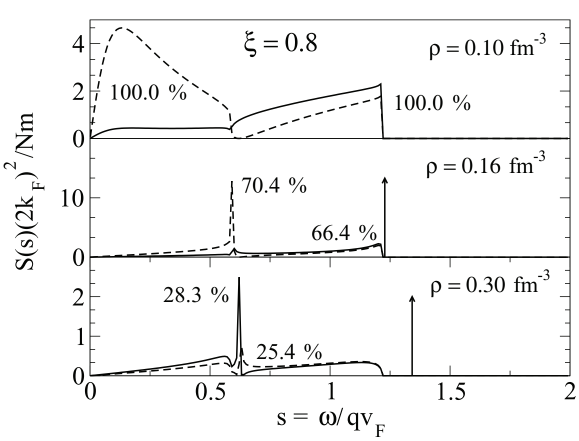

FIG. 6. Same as in Fig. 5 at isospin asymmetry $\xi = 0.8$.

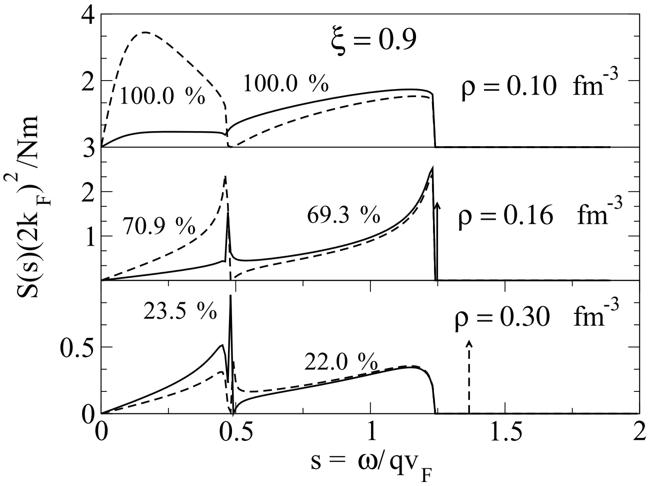

FIG. 7. Same as in Fig. 5 at isospin asymmetry $\xi = 0.9$.

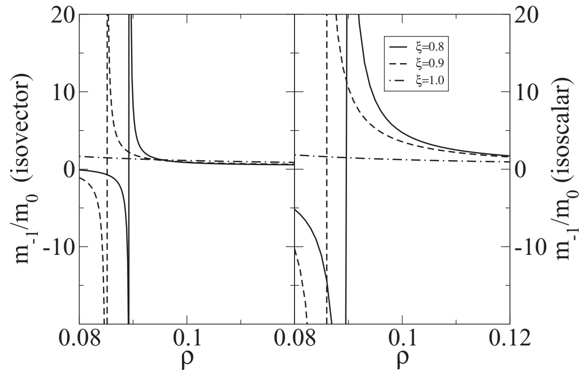

FIG. 9. Isoscalar and isovector compressibility ratios m^s_{-1}/m^0_{-1} and m^v_{-1}/m^0_{-1} as a function of the density ρ for values of ξ close to 1.

collective mode disappears in the isoscalar channel, due to Landau damping.

The situation is similar, but not exactly the same, in the case of pure neutron matter ($\xi = 1$). At high density ($\rho = 0.3$ fm^{-3}) the dynamic form factor shows a strong collective state of elastic nature at $\bar{s} = 1.3907$, exhausting about 81.4% of the energy-weighted sum rule, together with a continuum of single-particle excitations at lower s values. Decreasing the density to $\rho = 0.16$ fm^{-3}, the energy of the collective state decreases, likewise the percentage of the m_1 sum rule exhausted by this state. Eventually, at some density below $\rho = 0.16$ fm^{-3}, the collective completely decays in one-particle–one-hole excitations.

When $N \neq Z$, isoscalar and isovector probes excite an admixture of isoscalar and isovector modes. In all cases we predict a single collective state, when present, having different weights in m_1 for the isovector and isoscalar channels.

The neutron star core is supposed to be largely made up of neutrons, with the presence of a small quantity of protons.

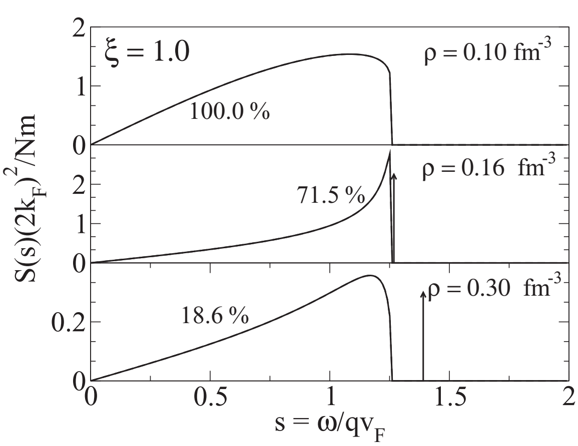

FIG. 8. Same as in Fig. 5 at isospin asymmetry $\xi = 1$. In this case, pure neutron matter, there is only one type of excitation and the distinction between isoscalar and isovector channels does not apply.

This situation corresponds to a value of ξ close to 1. Rather than considering the proton fraction predicted for each value of the density by the AFDMC equation of state, we have considered the cases $\xi = 0.8$ and $\xi = 0.9$ for all densities, in order to have an idea of the evolution of the collective modes with this parameter. For such values of the asymmetry, a clean collective state in both channels is present only at high density, where it exhausts about 70%–80% of the m_1 sum rule. Already at saturation density $\rho = 0.16$ fm^{-3}, this state has almost completly decayed into particle-hole excitations, since it exhausts only about the 30% of the m_1 sum rule in both channels. At $\rho = 0.10$ fm^{-3} it is completely damped. This suggests that collective modes in the isoscalar or isovectors channels can be present going inward from the interface between the inner crust and the outer core.

Another interesting analysis can be made by looking at the compressibility (in units of the compressibility of the free Fermi gas) as a function of the density for different values of the proton fraction. This quantity is given by m^s_{-1}/m^0_{-1} and m^v_{-1}/m^0_{-1}, and is plotted in Fig. 9. It can be noticed that a strong divergence for a density near $\rho = 0.085$ fm^{-3} appears at $\xi = 0.9$, and that it moves to a larger density, increasing the proton fraction. We interpret this divergence as a sort of mechanical instability of matter towards the formation of an inhomogeneous phase, as expected in the inner crust of the neutron star.

It is also interesting to look at the regime that would correspond to asymmetries typical of neutron-rich nuclei close to the drip line, i.e. $\xi = 0.3$. At (unphysical) high density, a collective state exhausting about 50%–60% of m_1 at $\bar{s} = 1.2072$ is present both in $S^s(s)$ and $S^v(s)$. At the same time the quasiparticle-quasihole strength is practically concentrated in one state at a value of s slightly smaller than 1 and exhausting about 50%–40% of m_1. By lowering the density, we observe that at $\rho = 0.16$ fm^{-3} the collective state appears at a lower energy, and remains collective only in the isovector channel, where it still exhausts more than 60% of the energy-weighted sum rule. In the isoscalar channel most of the strength is taken by the one-particle–one-hole excitations, though concentrated in a narrow region of s, and the "collective" solution exhausts only about 17.8% of the m_1 sum rule. At $\rho = 0.10$ fm^{-3} the

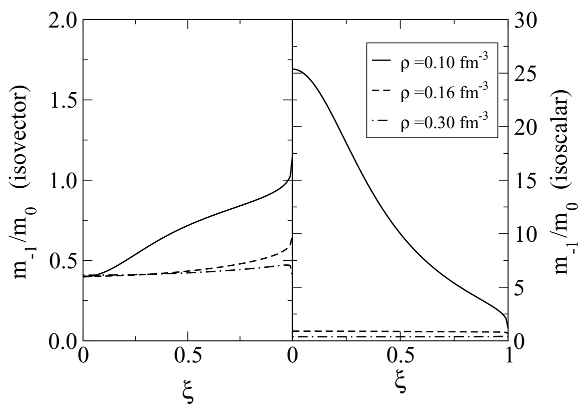

FIG. 10. Isoscalar and isovector compressibility ratios m^s_{-1}/m^0_{-1} and m^v_{-1}/m^0_{-1} as a function of the isospin asymmetry ξ for three different values of the density.

collective mode can be excited only by an isovector probe, and in the isoscalar channel it is practically completely damped. The quasiparticle-quasihole strength is distributed in a wide range of s in the isoscalar channel, whereas in the isovector one it continues to see a substantial concentration at $s \sim 1$.

This situation might be interpreted in analogy to what happens in nuclei with a large excess of neutrons, where a low-energy peak beyond the usual giant resonance is observed in the isovector channel.

Finally, in Fig. 10 we plot the compressibility ratio for three different values of the density. At $\xi = 0$ and $\xi = 1$, m^s_{-1}/m^0_{-1} gives the compressibility of symmetric nuclear matter and pure neutron matter, respectively. These values are not far from the results computed by other authors starting from a microscopic AV8′ Hamiltonian [20]. From the figures one also sees that, differently from what happens at low density, at normal and high densities m^s_{-1}/m^0_{-1} is practically independent of ξ. On the contrary, m^v_{-1}/m^0_{-1} turns out to be always an increasing function of the isospin asymmetry.

V. CONCLUSIONS

We have studied the dynamic form factor of asymmetric nuclear matter by using a time-dependent local isospin density approximation approach based on a local density energy functional derived by an auxiliary field Ddiffusion Monte Carlo calculation. The more relevant results we have found are the following:

(i) We find the presence of a strong collective state at high density at an energy which increases with the value of the nuclear asymmetry $\xi = (N - Z)/A$. By decreasing the density to the saturation value ($\rho = 0.16$ fm^{-3}), this state tends to decay in quasiparticle-quasihole states. The decay is faster in the isoscalar channel, where it remains very collective only at values of ξ close to 0. When the density is further decreased, the collective states survives only in the isovector channel at small values of ξ, typical of the neutron star interior.

(ii) When a small fraction of protons is added to neutron matter, when ξ is equal to 0.8, 0.9, and at values of the density near or slightly smaller of 0.09 fm^{-3}, the system becomes unstable. This instability is seen in the isoscalar and isovector compressibilities, which at such densities diverge.

(iii) When ξ is around 0.3 (small asymmetry), in the isovector channel at all the densities two states cohexist, one of collective and the other of quasiparticle-quasihole nature, practically sharing the fraction of exhausted energy-weighted sum rule. This is similar to what is observed in the photodisintegration of large neutron-excess nuclei.

ACKNOWLEDGMENTS

We thank W. Leidemann and G. Orlandini for useful discussions about the subject of the paper. F.P. is a member of LISC, Interdisciplinary Laboratory for Computational Science, a joint venture of the University of Trento and of the Bruno Kessler Foundation.

[1] R. F. Sawyer, Phys. Rev. D **11**, 2740 (1975).
[2] R. F. Sawyer, Phys. Rev. C **40**, 865 (1989).
[3] N. Iwamoto and C. J. Pethick, Phys. Rev. D **25**, 313 (1982).
[4] A. Burrows, S. Reddy, and T. A. Thompson, Nucl. Phys. A **777**, 356 (2006).
[5] N. Chamel and P. Hansel, Living Rev. Relativity **11**, 10 (2008).
[6] C. J. Horowitz, M. A. Pérez-García, J. Carriere, D. K. Berry, and J. Piekarewicz, Phys. Rev. C **70**, 065806 (2004).
[7] C. J. Horowitz, M. A. Pérez-García, D. K. Berry, and J. Piekarewicz, Phys. Rev. C **72**, 035801 (2005).
[8] C. Shen, U. Lombardo, N. Van Giai, and W. Zuo, Phys. Rev. C **68**, 055802 (2003).
[9] O. Benhar, A. Cipollone, and A. Loreti, Phys. Rev. C **87**, 014601 (2013).
[10] K. E. Schmidt and S. Fantoni, Phys. Lett. B **446**, 99 (1999).
[11] S. Gandolfi, A. Yu. Illarionov, S. Fantoni, J. C. Miller, F. Pederiva, and K. E. Schmidt, Mon. Not. R. Astron. Soc. **404**, L35 (2010).
[12] A. Akmal, V. R. Pandharipande, and D. G. Ravenhall, Phys. Rev. C **58**, 1804 (1998).
[13] S. Gandolfi, A. Yu. Illarionov, F. Pederiva, K. E. Schmidt, and S. Fantoni, Phys. Rev. C **80**, 045802 (2009).
[14] H. DJapo, B. J. Schaefer, and J. Wambach, Phys. Rev. C **81**, 035803 (2010).
[15] J. P. Perdew, Phys. Rev. B **33**, 8822 (1986).
[16] Ll. Serra and E. Lipparini, Europhys. Lett. **40**, 667 (1997).
[17] W. Kohn and L. J. Sham, Phys. Rev. **140**, A1133 (1965).
[18] E. Lipparini, *Modern Many-Particle Physics* (World Scientific, Singapore, 2003).
[19] F. Dalfovo and S. Stringari, Phys. Rev. Lett. **63**, 532 (1989), and references therein.
[20] S. Fantoni, A. Sarsa, and K. E. Schmidt, Phys. Rev. Lett. **87**, 181101 (2001).